2010 IEEE International Conference on Robotics and Automation
Anchorage Convention District
May 3-8, 2010, Anchorage, Alaska, USA

Phased-Array Piezoelectric Actuators Using a Buckling Mechanism Having Large Displacement Amplification and Nonlinear Stiffness

Devin Neal, Harry Asada, *Member, IEEE*

Abstract—**Novel designs of an array of piezoelectric stack actuators using a unique buckling mechanism are presented in this paper. Multiple PZT actuator units with high gain displacement amplification mechanisms are arranged in parallel with spatial phase differences. Having an inherent kinematic singularity, the buckling mechanism provides not only an extremely high gain of displacement amplification, but also varying stiffness and nonlinear force-displacement characteristics. The phased array PZT actuator exploits this nonlinearity for gaining a large output displacement as well as for combining multiple PZT stacks in parallel without conflicting with each other. Three specific designs of arrayed buckling actuators are presented. The aggregate output force-displacement relationship is analyzed and its profile is shaped with respect to spatial phase differences and nonlinear stiffness and force characteristics of individual PZT buckling actuator units.**

I. Introduction

PIEZOELECTRIC actuators have a number of salient features, including high stress, high bandwidth, and high power density along with stable and reliable material properties. Despite valuable features, the greatest shortcoming of piezoelectric actuators is the limited strain they produce. Strains of PZT stacks are on the order of 0.1%, well below skeletal muscles and other smart structure materials. Displacement amplification has been a subject of piezoelectric actuator research for the past several decades. A number of methods have been developed, which can be classified into internally leveraged (bi-morph bending cantilevers, and uni-morph bowing actuators), externally leveraged (lever arm, hydraulic, and flextensional actuators), and frequency leveraged actuators (inchworm, and ultrasonic actuators) [1]. Internally leveraged actuators exhibit substantial displacement but with significantly decreased force due to the strain energy absorbed in bending and low stiffness. Frequency leveraged actuators rely on friction of contacting surfaces, which varies depending on pressure and surface conditions. Applications are limited to light duty, and open-loop repeatability is limited [2].

This paper focuses on a novel type of flextensional displacement amplification. Flexure based amplification methods have been studied extensively. They were originally designed for acoustic purposes, but have since been designed to maximize output deflection and force [3]. These actuators include the Moonie [4] and the Cymbal [5]. These designs are modular and have been stacked serially to increase net displacement [6]. Most of the flextensional mechanisms use a rhombus-type amplification structure. A single rhombus can produce approximately 10 times larger displacement. In an attempt to gain a larger effective strain, nested amplification mechanisms have been developed. Using two layers of the rhombus-type amplification, over 20% effective strain has been obtained, where the effective strain is defined to be the ratio of output displacement to actuator body length along the axis of output displacement [7].

This paper presents an alternative method, which can produce over 100 times larger displacement in a single stage. The key idea is to exploit "buckling", a pronounced nonlinearity of structural mechanics. While this nonlinear and singular phenomenon can produce an order-of-magnitude larger displacement amplification than typical flexure based methods, buckling is an unstable, unpredictable phenomenon. Nonlinear stiffness characteristics are not inherently negative though. For example, the unstable stiffness characteristics of a similar bi-stable element have been utilized to shape the force-displacement profile of dialectric polymer actuators [8]. Additionally, the unpredictability of buckling can be controlled. In our previous publication, a method for controlling the direction of buckling was first developed by using an additional mechanical stiffness, and asynchronously activating a pair of independent piezoelectric stacks [9].

This paper extends the buckling concept to multi-unit arrayed actuators. The arrayed buckling actuators not only control the buckling direction, but also produce higher force and larger displacement by arranging multiple PZT units in an array. The basic buckling actuator concept is reviewed, followed by several arrayed design concepts.

II. Principle And Design Concept [9]

Fig. 1 shows the schematic of a nonlinear, large-strain buckling piezoelectric actuator, consisting of a pair of piezoelectric stacks and a monolithic structure. The monolithic structure mechanically grounds the piezoelectric stacks between a "keystone" output node and the end supports placed at both sides. The end supports, and output node are connected to the piezoelectric stacks through rotational joints.

As the PZT stacks are activated, they tend to elongate, generating a large stress along the longitudinal direction. When the two PZT stacks are completely aligned, the longitudinal forces cancel out, creating an unstable

Manuscript received September 15, 2009.

D. M. Neal is with MIT, Cambridge, MA 02139 USA (phone: 415-260-4634; e-mail: dneal@mit.edu).

H. H. Asada is with MIT, Cambridge, MA 02139 USA.

equilibrium. With any disturbance, the two PZT stacks tend to "buckle" as illustrated in Fig. 1(b). Let Δl be the elongation of each PZT stack and y be the vertical displacement of the keystone output node. The displacement amplification ratio, $G = \frac{\Delta y}{\Delta \ell}$ tends to infinity as y approaches 0. Differentiating the kinematic relation, $y^2 = (L + \Delta l)^2 - L^2$, in terms of $\Delta \ell$ and ignoring higher-order small quantities yields the following amplification ratio, G,

$$G \cong \frac{L}{y} \to \infty, \text{ as } y \to 0 . \quad (1)$$

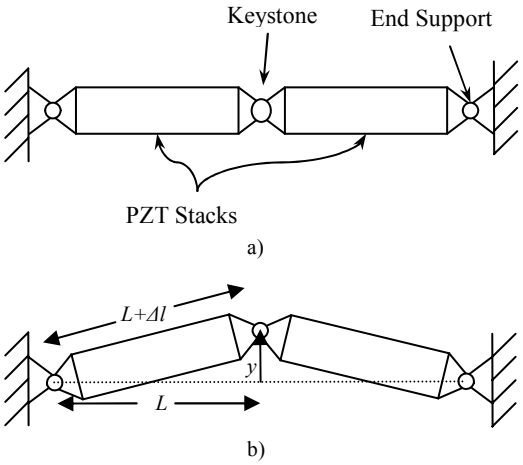

Fig. 1. Kinematics without redirecting stiffness.

This is a type of kinematic singularity. Even for a finite piezoelectric displacement, the amplification gain, G, is significantly large. Although this buckling mechanism can provide extremely large displacement amplification, buckling is in general an unpredictable, erratic phenomenon, which is difficult to control. We do not know which direction the output node will move, upward or downward. It is also not feasible to quasi-statically bring the output keystone from one side to the other across the middle point. Once it goes upwards, it tends to stay there, and vice versa. This is in a sense "mono-polar" activation where the stroke of the output keystone is half of the total possible displacement. Therefore, it is desirable to both control the buckling direction, and have the capability to pass through the singularity point to the other side once buckling has occurred. To achieve this "bi-polar" activation, previous methods have utilized additional mechanical stiffness elements [9]. This paper presents an alternative approach: multiple buckling actuator units are arranged in parallel with spatial phase differences among the units. This utilizes nonlinear kinematic and static properties of buckling which are analyzed next.

III. Kinematic Model of a Single Unit

To analyze the quasi-static performance of a single buckling unit, we model the actuator as a system of two springs as shown in Fig. 2.

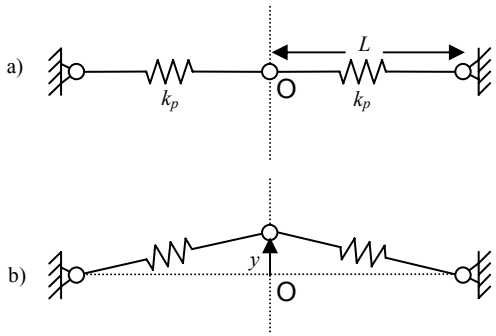

Fig. 2. Simplified static model of PZT buckling mechanism at a) singularity point (y=0) and b) at finite displacement (y≠0).

The stiffness of the springs, k_p, is determined by the series stiffness of the piezoelectric actuator and compressive stiffness of the joints. The inactive rest length of the springs is L, and the active rest length of the each spring is $L+\Delta l$, where Δl is the free displacement at the given activation level. With this model, the potential energy in each spring is equal to $\frac{1}{2}k_p\delta^2$, where δ is the deviation from rest length of the spring as a geometric function of displacement, y, and activation free displacement, Δl. Additionally, the rotational stiffness of the flexures is taken into account, and the energy in them is dependent on the square of the change in bending angle. We calculate the potential energy, U, of the system of springs, at various activation levels as a function of the output displacement, as shown in Fig.3, where the activation level means the ratio of applied voltage to the maximum applicable voltage across the PZT stacks. The force, F, in the output direction can be found by calculating $-dU/dy$, and the stiffness can be found by calculating d^2U/dy^2. The stiffness and force are plotted in Fig. 3 for a prototype actuator using commercially available PZT stacks [10].

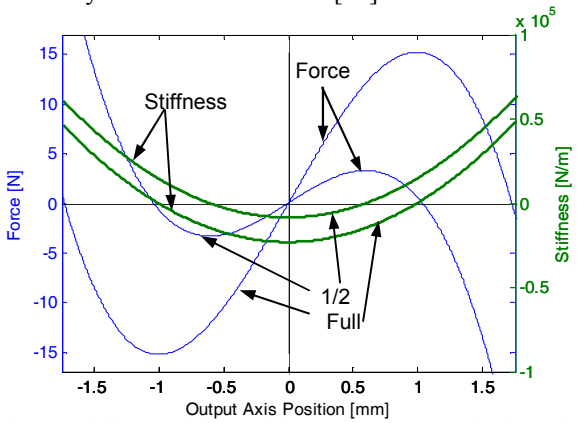

Fig. 3. Stiffness and force of the actuator output node along the output axis as a function of output node position for two activation levels: 1/2, and full activation.

There are a few important features to note about a single buckling actuator that can be seen in Fig. 3.

1) *The significant displacement amplification of the actuator.* The displacement in a single direction is greater than 1.5 mm at full activation, i.e. 150 V. Compared to the maximum free displacement of the PZT stack (15 µm) at 150 V, this buckling actuator produces 100 times larger displacement [10].

2) *Nonlinear force-displacement characteristics.* The maximum force is generated not at the zero-displacement ($y = 0$), but at a middle stroke. In turn no force is generated at the singular point at $y = 0$.

3) *Varying stiffness.* Near the singular point, the stiffness is zero or negative, whereas it increases sharply as displacements get larger in both directions.

The second feature 2) above significantly differs from the inherent PZT stack properties and the properties of conventional strain amplification mechanisms, where the peak force, i.e. blocking force, is created when no displacement is made. The output force decreases monotonically, as displacement increases. In contrast, the buckling actuator produces its peak force mid-stroke. This nonlinear force-displacement relationship is useful, as we exploit later in designing multi-unit actuators.

Furthermore, the buckling actuator exhibits a unique stiffness characteristic; stiffness becomes zero, or even negative with non-zero activation level, in the vicinity of the singular point. This is useful for arranging multiple units in an array. When one unit moves in the vicinity of the singular point, it is effectively "disengaged" from other units, so that it may not be a "load" for the other units producing forces. Using these features of buckling actuators, we have designed multi-unit actuators with minimal mechanical conflict for achieving large bi-polar displacement and improved force-displacement characteristics.

IV. Dual-Unit Translational Buckling Actuator

A. Phased Array Actuation

Consider two buckling actuator units arranged in parallel, as shown in Fig. 4. We know that a single unit buckling actuator can essentially disengage from the system it is in when near the singularity point, so it is similarly possible to mechanically couple the output nodes of two units and have them interfere very little with each when each is near its singularity point. If the two units are in phase as in Fig. 4(a), then each unit is only disengaged when the other is as well. With this in-phase orientation, the actuator does not take advantage of a single unit's ability to disengage from the other. However, if the two units are out of phase as in Fig. 4(b), then when one unit is near its singularity point, the other is capable of producing much greater force. Thus, when one unit can effectively disengage, the other unit can still influence the output load.

If the inactive equilibrium angle, θ_0, (shown in Fig. 4(b)) is small enough then the bucking direction of the pair of units can be controlled. This is demonstrated in Fig. 5. At t_1, both units are inactive in both a) and b). Control is possible if activating one unit and not the other will force the inactive unit's output node through its singularity point. In Fig. 5, at time t_2, one unit is activated; the bottom unit for a) and the top unit for b). In both cases, the active unit has forced the inactive unit through its singularity position. Once the output nodes of both units are on the same side of their respective singularity points, activating both causes further displacement, as seen at time t_3 in Fig. 5. This requires the top and bottom pairs to be activated asynchronously or temporally out of phase. Fig. 5 demonstrates that this phased activation can move the output nodes up or down. Thus the phased array actuator utilizes both being out of phase spatially and being activated out of phase temporally.

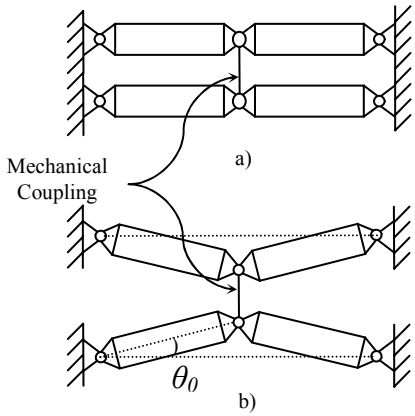

Fig. 4. Diagrams of dual-unit buckling actuators a)spatially in phase, and b) spatially out of phase.

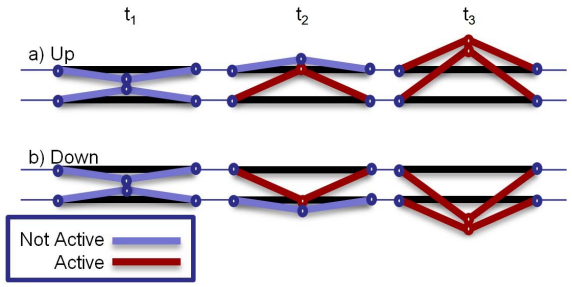

Fig. 5. Asynchronous activation time sequence of dual-unit phase-shifted buckling actuator, showing a) upwards free displacement, and b) downwards free displacement.

B. Dual-Unit Actuator Simulation

As with the simulation for the single unit buckling actuator, the series stiffnesses of the piezoelectric actuators and axial stiffness of the joints were modeled as springs, while the activation levels of the piezoelectric actuators were modeled as effectively changing the rest length of those springs. Additionally, the bending stiffness of the flexures were modeled as rotational springs. The potential energy values for three activation scenarios are shown in Fig. 6. The graphs show the potential energy with two different values of the rest angle, θ_0; 0.3 degrees and 1.0 degrees.

When both units are inactive, as in Fig. 6(a) there is a single potential energy well at zero displacement. Regardless of the output position, there is a restoring force to the zero displacement position. This means that even if the output node of one of the units was extended beyond its singularity point, the actuator would still provide a restoring force to the zero displacement position. This is true regardless of the rest angel, θ_0.

When a single unit is active, as in Fig. 6(b), there is a nonzero slope in the potential energy function at a

displacement value of zero. This means that at the rest position, the output nodes will be forced in one direction. Notice that in Fig. 6(b) for θ_0 = 1.0 degrees, there is only one energy well, indicating that there exists just one unforced stable position. This is because this particular configuration was designed such that there would always be force toward a preferred side of the rest position. However, it is possible to have a design that would generate two energy wells, one on either side of the rest position, if the rest angle, θ_0, is smaller. This is the case in Fig. 6(b) for θ_0 = 0.3 degrees. Although, even with two equilibrium positions, the slope of the energy curve at the rest position is still nonzero, and the output would be forced in a preferred direction if it were at the rest position. By using a design with just one energy well, more control over the output is achieved, but at the cost of efficiency because a greater amount of energy from the input actuators is converted to strain energy within the actuator when both are activated as seen in Fig. 6(c).

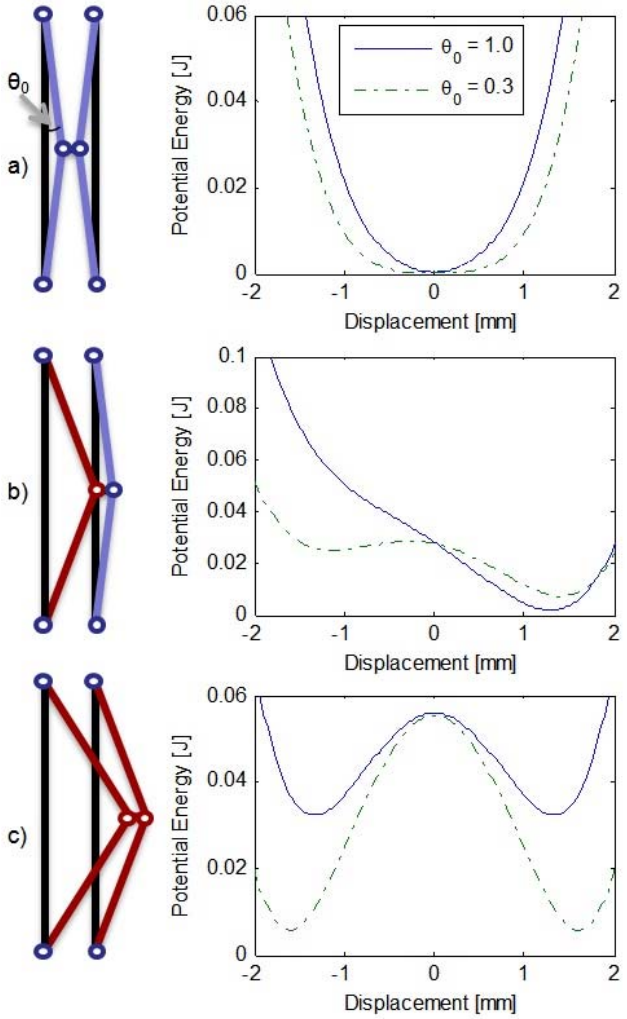

Fig. 6. Potential energy vs. displacement simulation plots of dual-unit out-of-phase actuator when a) neutral, b) left unit active, and c) both units active.

When both units are active, two symmetric unforced equilibrium points exist. These equilibrium displacements are greater in magnitude than the equilibrium point of greatest magnitude (whether 1 or 2) from activating just one unit. Also the maximum force is greater with both units active than with just one unit active. This can be seen by observing that the maximum negative mid-stroke slope in Fig. 6(c) is greater than the maximum negative mid-stroke slope of Fig. 6(b). Thus, the simulation shows that activating one unit, followed by the other after the output is beyond the zero displacement point, is a method of controlling the buckling direction of the actuator.

C. *Dual-Unit Phase-Shifted Actuator Implementation*

To demonstrate the degree of control granted by including two buckling units and using asynchronous activation, a dual-unit phase-shifted prototype was designed, built, and tested. It is shown if Fig. 7.

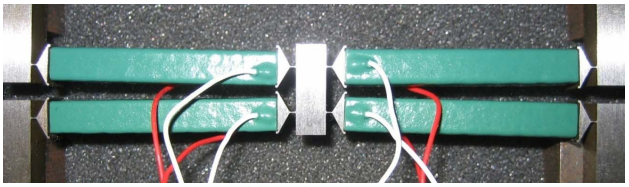

Fig. 7. Dual-unit phase-shifted buckling actuator prototype.

The graph of the output displacement in Fig. 8 shows the performance when using asynchronous activation with zero load. First the bottom unit is activated generating greater than 1 mm of displacement, followed by the top unit generating a total of about 2.5 mm of displacement. The top unit then is deactivated, followed by the bottom unit. Then the order of activation is reversed and repeats generating similar displacements. The multi-unit phase-shifted actuator consistently generates 4.9 mm of peak-to-peak free displacement. This design was specified to generate just one equilibrium position when one unit is active, as with θ_0 =1.0 in Fig. 6, to give a large degree of control. If the rest angle, θ_0, were to be decreased, output performance would increase but at the expense of robust directional control.

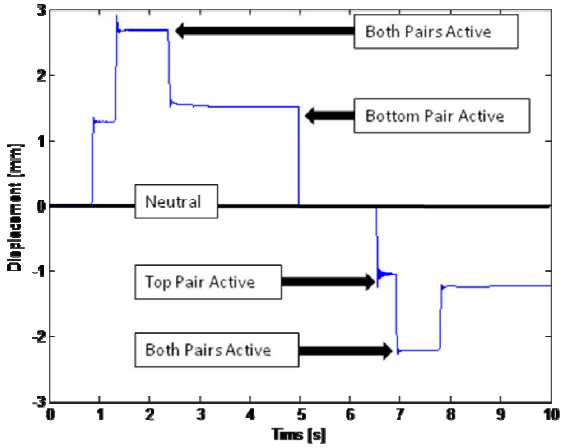

Fig. 8. Output free displacement performance of multi-unit phase shifted prototype.

V. Multi-Unit Translational Buckling Actuator

Spatially distributed multiple buckling units can generate translational motion when the multiple units are coordinated.

Fig. 9(a) illustrates an existing mechanism, where a group of linear actuators engaged with a wavy track push the surface in a coordinated manner. The output stroke of the system is limited only by the length of the track, and not the stroke of the individual input actuators. A thrust can be generated in the horizontal direction as the actuators are synchronized in phase with the wave location. This principle can be applied to the buckling actuators, as shown in Fig. 9(b) and (c).

A single buckling unit is diagramed simply as an output node that can move up and down in Fig. 9(b). In Fig. 9(c), the output of each buckling actuator moves up and down, within a track that is constrained to move horizontally. Because the output nodes are engaged with the track, but free to slide within it, the track is forced right or left by the buckling units up or down motion. For the half period section of track shown, upwards force from the buckling units will force the track to the right in the direction labeled "Track Direction."

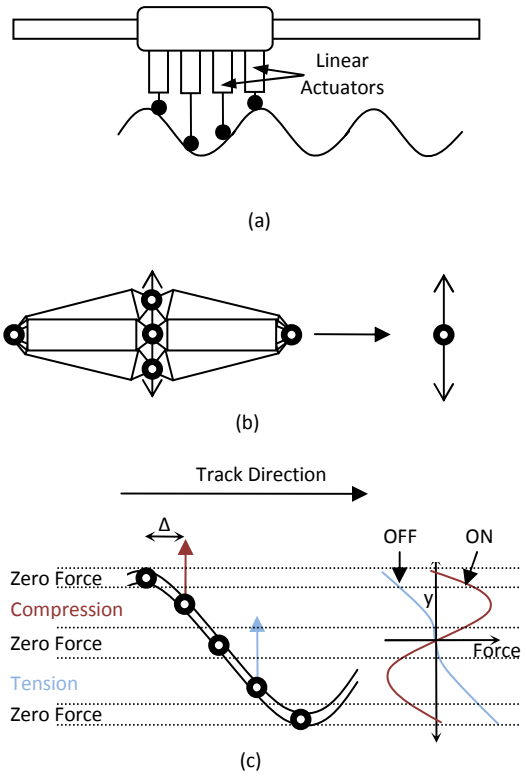

Fig. 9. (a) Multiple linear actuators used to generate continuous translational motion. Multiple buckling units with (b) a simplified diagram, (c) used to drive a track constrained to move perpendicular to the axes the buckling units move in.

By using multiple units, the units can provide a net thrust on the track at any distance the track has moved, and assist each other in passing through respective singularity points.

There are 4 types of zones that are repeated cyclically along the track that are shown in Fig. 9(c). Next to the track in Fig. 9(c), there is a plot of the force each buckling unit can impart on the track as a function of its position *y* for both the active ON and inactive OFF states. By looking at the force plot and track diagram, we can see two types of zones along the track at which the buckling units cannot produce thrust, and have been labeled as "Zero Force." One zone occurs when the buckling unit is near its singular position in the middle of the track. Recall that the buckling actuator cannot produce a force at the singular position. The other "Zero Force" zone type occurs at the buckling unit's maximum displacement where the rail has zero slope and cannot be forced left or right by a buckling unit. The two other zones are high force zones. The one labeled "Compression" in Fig. 9(c) is where a buckling unit is actively in compression, forcing away from its singularity position. The other type labeled "Tension" is where an inactive buckling unit is in tension, forcing towards its singularity position. Note that an inactive buckling unit can go through its singular position, since it is engaged with the track that pushes the inactive unit across the singular position. These forcing zones flip from compression to tension and vice versa when the forcing direction on the track is reversed.

It is necessary to be able to force the track in either direction at all possible track positions. This is accomplished by phasing the position of the buckling units along the track by a distance Δ as shown in Fig. 9(c). The compressive zones are repeated along the track twice for every period of the track. So for 4 units, the phase shift is 1/8 + n/2 times the periodic length of the track, where n is any integer. This phase shift ensures that one unit is in each of the 4 zones described above for all position of the track. Thus, the buckling units are capable of forcing the track for all track positions. The track progresses left or right depending on the temporally phased activation of the buckling units.

The performance of this phase arrayed multi-unit track actuator was simulated. Potential energy based simulation is again used to generate the force displacement relationship in Fig. 10. For this simulation, we assume ideal force transmission from the buckling units to the track. This means assuming the track is very stiff compared to the buckling units and does not store strain energy, and that friction is neglected. We also assume zero tensile force from the buckling units is contributed to the net force on the track. We also assumed a track with a constant slope of one, however altering the shape of the track can be used to shape the output force-displacement relationship for specific applications.

As the track progresses, the 4 buckling units transition into their next respective zones. Since one unit is in each zone at all track positions, the force-displacement curve repeats for each transition. A transition occurs for every 1/8 of a period length of the track.

Only units in the "compression" zones contribute force to the track. As one unit leaves a compression zone, another unit enters a compression zone. Therefore the net force on the rail is the combination of two buckling units at any given time as shown in Fig. 10. The curve gradually rising is the force contribution of the unit entering a high force "compression" zone, and the curve that drops to zero force is

the force contribution of the unit leaving the high force "compression" zone.

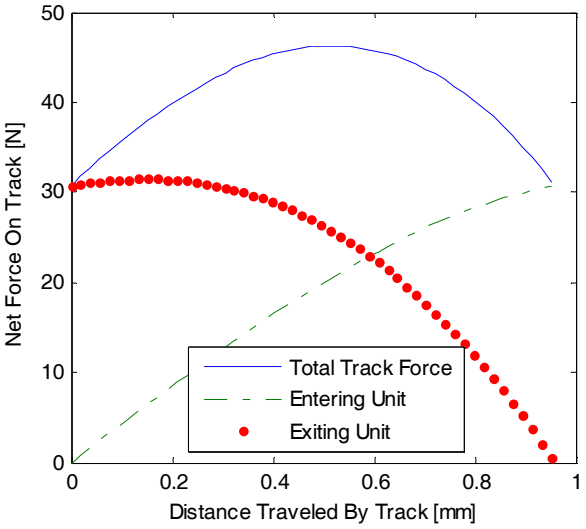

Fig. 10. Simulation of one period of the force displacement relationship for the multi-unit translational buckling actuator.

The simulation in Fig. 10 shows us that there is a force ripple as the track progresses. This ripple is repeated 8 times per period of the track, once for each time the units enter a different zone on the track. This ripple can be shaped in two ways. First, the shape of the track can be something other than a constant slope as simulated. The instantaneous track slope is the value of the force transmission ratio from a buckling unit to the track. Secondly, more buckling units could be used to decrease the relative magnitude of the ripple, and increase the ripple frequency.

VI. Multi-Unit Rotational Buckling Actuator

The straight track with periodic ripples utilized in the previous translational actuator design may be replaced with a recirculating track with periodic ripples utilized in a rotational actuator design as shown in Fig 11. Such a rotational actuator is capable of continuous rotational displacement. The method of applying force to the rotational track of Fig. 11 with multiple buckling units is identical to the method used for the translational track as diagramed in Fig. 9(c).

Multiple buckling units are positioned around the track with a phase shift equal to half the ripple period divided by the number of units used. At this point, the rotational track may be thought of as a rigid gear.

This rotational actuator bears many similarities to the harmonic drive gearing mechanism. A harmonic drive consists of a wave generator driving a flex spline within a rigid circular spline. Similarly, the rotational buckling actuator has a rigid internal spline/track with buckling units providing a flex-spline-like interaction with the internal spline. Instead of being driven by a wave generator, the buckling units are activated with specified temporal phase shifts to generate the wave-like motion along the rigid internal gear.

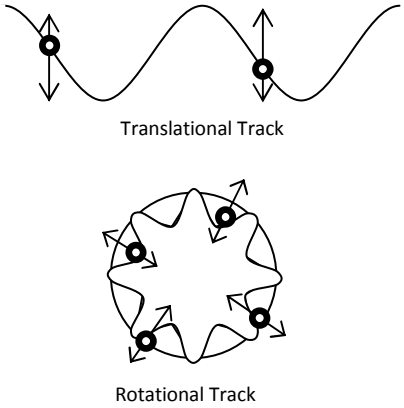

Fig. 11. Translational and rotational tracks for continuous motion multi-unit buckling actuators.

A solid model of the multi-unit rotational buckling actuator was created and tested in a simulation environment. The actuator shown in Fig. 12, consisted of 8 buckling units driving a rigid internal track constrained to freely rotate. The output nodes of the buckling units were constrained to follow the track. The track has an oscillation period of ¼ π radians. The buckling units are phase shifted by 1/16 of the track period. 1/16 of the track period in this case is 1/64 π radians.

In Fig. 12, we see the phase arrayed buckling units surrounding the rotational track/gear. Each buckling unit is making contact with the gear near the middle of the gear shaft. If the buckling unit support plates are grounded and the gear shaft is free to rotate, then the gear shaft will be rotated by the temporally phased activation of the buckling units. Notice also that the gear shaft in Fig. 12 is hollow. This hollow space within the actuator may be useful for any number of application specific reasons.

As seen in Fig. 13, a torque ripple similar to the force ripple of the translational actuator occurs. This ripple can similarly be shaped and mitigated by shaping the gear and/or incorporating more buckling units. Notice that the ratio of the torque ripple to the mean torque in Fig. 13 is much smaller than the ratio of the force ripple to the mean force in Fig. 10. This is because there are 8 units acting out of phase rather than just 4.

Utilizing multiple buckling units in this harmonic-drive-like mechanism is promising because of the favorable tradeoff of frequency for displacement. This rotational actuator is a frequency leveraged device because the PZT input actuators are activated at a frequency much higher than the output rotation frequency. With the 8 period/tooth gear used in the model and simulation, the buckling units must cycle 8 times for one revolution of the output shaft. The natural frequency of a single buckling unit of the type simulated in the rotational actuator was found to be more than 50 Hz [9]. This means an output rotational frequency of 6.25 Hz.

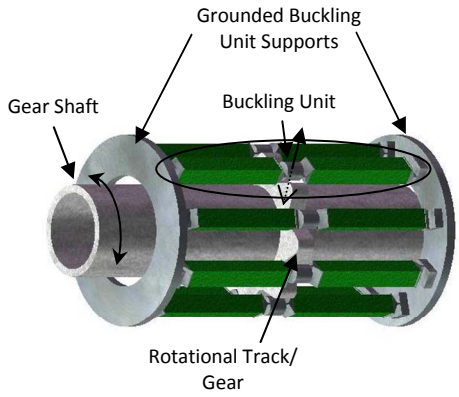

Fig. 12. Rendering of multi-unit phase shifted rotational buckling actuator.

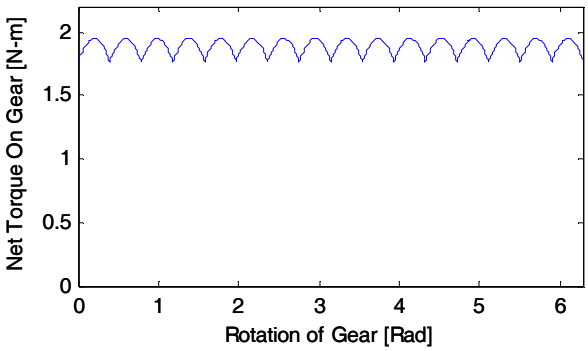

Fig. 13. Output performance of rotational buckling actuator along a full cycle of rotation.

VII. Conclusion

Large displacement amplification in a single amplification step has been realized through utilizing a singular buckling phenomenon. What we have demonstrated in this paper is that this buckling can be exploited and controlled using multiple units if they are spatially phased and temporally phased when actuated. By making use of spatial and temporal phasing, three significantly different actuator designs were created. A dual-unit buckling actuator prototype was built and tested that is capable of generating nearly 5 mm of peak-to-peak displacement from input actuators only capable of 44 µm. A multi-unit translational actuator that is capable of continuous linear displacement was designed and simulated. Lastly, a rotational actuator, similar to a harmonic drive, which allowed for continuous rotational motion without relying of friction, was modeled and simulated. For comparison, the driving module of commercially available ultrasonic piezoelectric linear drives achieve a power-to-volume ratio nearly identical to the power-to-volume ratio of the input actuators of the translational actuator described in this paper; 2.5e5 W/m^3 [10]. The multi-unit continuous drives described in the paper are better suited to larger force, and faster displacement than typical commercially available ultrasonic drives. The future direction of this research is to develop the harmonic-drive-like actuator to perform in the design subspace between piezoelectric ultrasonic motors and large displacement piezoelectric actuators.

References

[1] C. Niezrecki, D. Brei, S. Balakrishnan, and A. Moskalik, "Piezoelectric Actuation: State of the Art," *The Shock and Vibration Digest*, 33 (4), 2001, pp. 269-280.

[2] Physik Instrumente, *Piezo Nano Positioning Inspirations 2009*, pp. 1-24-1-29.

[3] W. Touli, "Flexural-extensional electromechanical transducer," 1966. US Patent 3,277,433.

[4] R. Newnham, A. Dogan, Q. Xu, K. Onitsuka, J. Tressler, and S. Yoshikawa, "Flextensional Moonie Actuators," *In 1993 IEEE Proceedings. Ultrasonics Symposium*, vol. 1, 1993, pp. 509–513.

[5] A. Dogan, K. Uchino, and R. Newnham, "Composite piezoelectric transducer with truncated conical endcaps 'Cymbal'," *IEEE Transaction on Ultrasonics, Ferroelectricsand Frequency Control*, vol. 44, no. 3, 1997, pp. 597-605.

[6] K. Onitsuka, A. Dogan, J. Tressler, Q. Xu, S. Yoshikawa, and R. Newnham, "Metal-Ceramic Composite Transducer, the 'Moonie'," *Journal of Intelligent Material Systems and Structures*, vol. 6, no. 4, 1995, p.447.

[7] J. Ueda, T. Secord, and H. Asada, "Static lumped parameter model for nested PZT cellular actuators with exponential strain amplification mechanisms," in *IEEE International Conference on Robotics and Automation,* 2008. pp. 3582-3587.

[8] A. Wingert, M Lichter, S. Dubowsky, "Hyper-Redundant Robot Manipulators Actuated by Optimized Binary Dielectric Polymers," in *Proceedings of SPIE,* vol. 4695, 2002, pp. 415-423.

[9] D. Neal, H. Asada, "Nonlinear, Large-Strain PZT Actuators Using Controlled Structural Buckling," in *Proceeding of the IEEE International Conference on Robotics and Automation*, 2009. to be published.

[10] Thorlabs.com, "Piezo-electric actuators," August 2009.